A NUMERICAL STUDY OF THE TEAR FILM RUPTURE

ASAD A. SALEM
College of Science and Technology
Taxes A&M University-Corpus Christi
Corpus Christi, TX 78412

Abstract: The drainage of the precorneal tear film in humans is studied. A fluid dynamic model for the drainage of the aqueous layer is developed that includes rheological effects. The Ostwald de Waele type power law model is employed to model the tear film. The nonlinear evolution equation for the film is formulated using the balance equations including a body force term due to van der Waals molecular attractions, lubrication theory and perturbation expansion method. The governing equation was solved by Lax-Wendroff finite-difference technique as part of an initial value problem for spatial periodic boundary conditions. The results indicate that the rheological effects of the tear film fluid affect the film drainage process and therefore be included in models for tear film damage.

Key-Words:- Tear film, Lubrication theory

1. Introduction

The human tear film is described as consisting of three distinct layers. A mucous layer lies on top of the epithelial cells of the cornea; an aqueous layer is present above the mucus layer and a lipid or fatty layer covers the aqueous layer. When the lids close, the lipid layer is compressed between the lid edges and its thickness increases. When the lids are half closed, the lipid layer is thick enough to exhibit interference colors. When the lids are completely closed, the liquid layer is about 0.1 micrometers thick. This is thin enough for the lipid layer to remain confined between the lid edges; consequently, lipid epiphora does not occur. It is important to note that in normal eyes, the lipid layer does not penetrate under the lids during blinking. The aqueous tear layer contains electrolytes, enzymes and various other proteins and glycoproteins. The ocular Surface, often referred to as the mucin layer, is about as thick as the superficial lipid layer and does two things:

i. makes the surface lacrophillic and
ii. maintains this lacrophilicity by masking entrapped lipid molecules.

Due to the small thickness of the tear film (10 micrometers, about 1/5th of the diameter of a strand of hair) the following things are true:

1. The tear film can only remain continuous if the ocular surface is and remains lacrophilic. More accurately, the film energy (sum of the energies associated with its outer and inner boundaries) has to be less than free energy of the ocular surface. In the eye this is achieved by lowering the energy (tension) at the mucin/aqueous tear interface and lowering the energy (tension) of the superficial lipid layer (mucin-lipid interaction) so the sum of these two is minimized.
2. Gravitational forces on such a thin film are negligible when compared to surface forces. This is why tear film does not flow downward when one is standing. However, the normal tear meniscus is deep enough for hydraulic (gravity-driven) flow to take place.

The viscosity of aqueous tears is only slightly higher than water which allows the tear layer under the lipids to perform as an excellent lubricating layer during blinking. During blinking, only the superficial lipid layer is eliminated. The aqueous tear layer remains under the lid where it is bound on both sides by the conjunctiva (and at one location by the cornea) in the closed eye. It provides hydrodynamic lubrication as long as it remains stable. When the eye lids are lax and floppy, or where the globe (cornea) and lid congruity is compromised, problems can arise. As the eye lid opens, the lipid layer spreads upward. Underneath the forming lipid layer the associated sialo-mucin also spreads upward thereby further stabilizing the lipid layer. This process thickens the tear film somewhat and it is completed in about one second. The tear film thickening process is governed by the tear meniscus which serves as a reservoir. The superficial lipid layer retards evaporation and protects the tear film from the invasion of the skin lipids (highly polar, they would be capable of rupturing the tear film and de-wetting the eye) contributing to stability by providing a low energy surface. Even in the normal open eye some of the lipid molecules will migrate to the mucin layer thereby corrupting its lacrophilicity. Due to the lipid-masking ability to mucin, considerable amount of lipid is needed to achieve lacrophilicity. The speed of the process depends on the tear film thickness. When one omits blinking (e.g. during staring) the tear film will eventually rupture forming dry spots at several locations thereby irritating the eye. Blinking rejuvenates the lacrophilicity of the ocular surface and removes heavily contaminated mucin, usually in the form of threads, to the lower formix. Thus, dry spot formation can happen in people with healthy eyes and normal tear film. All it takes is to refrain from blinking for more than 30 seconds or even a minute or two. It depends also on the environment. Turbulent, relatively dry air (air condition, on air planes) will accelerate the process.

Dry eye occurs because the ocular surface becomes lacrophobic, compromising the tear film's stability. The cause of the rupture of the tear film, often at several locations, is due to local nonwetting. If the tear film ruptures before the next blink and this happens repeatedly, the demise of the surface epithelium commences. An important quantitative clinical tool used by othalmologists to quantify dry eye conditions is the tear film break up time (BUT). The breakup of the tear film was first explained based on mucus interface due to the surface tension gradient driven motion called as the Marangoni effect, disrupting the mucin layer function of enhancing the wetting of corneal surface and consequently creating a highly hydrophobic surface [1]. The resulting distribution of lipids over the aqueous-mucus interface increases aqueous-mucus interfacial tensions, as the lipids are much less surface active than the mucus covering the epithelium, contributing stability to the tear film [2]. Furthermore, the Marangoni flow induces convective diffusion, preventing molecular diffusion of lipids to the corneal epithelium [3]. A Marangoni flow driven by mucin concentration was proposed, but is physically less likely in the presence of surface-active agents. Sharma and Ruckenstein [4] argued that the mucus is unstable due to the long range intermolecular dispersion.

2. Analysis

We consider the flow of a thin liquid film along a horizontal cylinder. We assume the characteristic thickness of the film to be ho and the length scale parallel to the film to be L. The aspect ratio is given by ζ=ho/L. If assume that $\zeta \ll 1$, we have a thin film. Assuming that the liquid is a power law fluid (Ostwald de Waele type), we may write:

$$\tau_{ij} = m\left|\gamma_{ij}\right|^{(n-1)}\gamma_{ij} \qquad (1)$$

where τ_{ij} is the stress tensor, γ_{ij} is the rate of strain tensor, n is the power-law exponent, and m is the viscosity index. We now use the following length scales:

Time: $\left[h_o\left(\rho h_o^n / m\right)\right]^{1/(n-2)}$

Length: $[\, h_0 \,]$

Velocity (U_o): $\left[\left(\rho h_o^n / m\right)\right]^{1/(n-2)}$

Pressure and stress: $\left[\rho\left(\rho h_o^n / m\right)\right]^{2/(n-2)}$

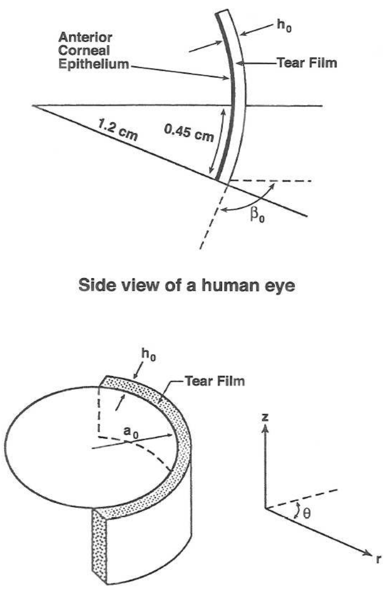

Fig.1. Flow model for the thin film flow.

The liquid layer is assuming thin enough that van der Waals forces are effective and thick enough that a continuum theory of liquid is applicable. Figure 1 shows the geometry of the eye. The dimensionless equation of mass, momentum, angular momentum equations are given by:

$$\frac{\partial u}{\partial x}+\left(\frac{1}{a+y}\right)\frac{\partial (a+y)v}{\partial y}=0 \qquad (2)$$

$$\frac{\partial u}{\partial t}+u\frac{\partial u}{\partial x}+\frac{\partial u}{\partial y}=-\frac{\partial p}{\partial x}+\frac{1}{(a+y)}\frac{\partial\left[(a+y)\left(\frac{\partial u}{\partial y}\right)^{n}\right]}{\partial y} \qquad (3)$$

$$0=-\frac{\partial p}{\partial y} \qquad (4)$$

In above dimensionsless equations, u and v represent the velocity components in x and y directions respectively, p the pressure and Ψ the potential function describing the van der Waals forces. We follow William and Davis [8] and write a modified expression for Ψ**:**

$$\psi = Ah^{-c} \qquad (5)$$

where c = 3 is usually used.

In equation (5), the van der Waals forces are represented through the potential function Ψ and A' is the dimensional Hamaker constant. A is related to the Hamaker constant A' as

$$A=\frac{A'}{6\prod \rho h_o{}^3 D} \;;\quad \text{where}$$

$$D=\rho\left(\rho h_o{}^n \big/ m\right)^{2/(n-2)} \qquad (6)$$

The boundary conditions along the solid plane wall are given by

$$y=0:u=v=0 \qquad (7)$$

At the fluid interface, we have the Kinematic condition:

$$y=h(x,t):\ \frac{\partial h}{\partial t}+u\frac{\partial h}{\partial x}=v \qquad (8)$$

The continuity of tangential stress on the interface requires

$$y=h(x,t):\frac{\partial u}{\partial y}=0 \qquad (9)$$

The continuity of normal stress at the interface y = h(x,t) becomes,

$$\frac{2\left[\left(\left(\frac{\partial h}{\partial x}\right)^2\frac{\partial u}{\partial x}+\frac{\partial v}{\partial y}\right)-\left(\frac{\partial u}{\partial y}+\frac{\partial v}{\partial x}\right)\frac{\partial h}{\partial x}\right]}{\left[1+\left(\frac{\partial h}{\partial x}\right)^2\right]}=-\frac{3S\left[\frac{\partial^2 h}{\partial x^2}-\frac{\left(1+\left(\frac{\partial h}{\partial x}\right)^2\right)}{(a+y)}\right]}{\left[1+\left(\frac{\partial h}{\partial x}\right)^2\right]^{3/2}}\text{-P} \qquad (10)$$

$$\text{where, } S=\left(\sigma \big/ 3h_0\right)D \qquad (11)$$

dimensionless surface tension. Our aim here is to solve for the stability of the liquid film while including the effect of van der Waals forces.

We now apply long wave theory to study the stability problem. When the layer is thinner than critical value, small disturbances begin to grow. These waves have wavelengths much larger than the mean thickness of the layer. Defining a small parameter κ that is related to wave number of such disturbances, we may rescale the governing equation by the order of magnitude considerations:

$$X = \kappa x \,;\; Y = y \,;\; \tau = \kappa^4 t \,;\; \psi_0 = \kappa^{-2}\psi$$
$$U = \kappa^{-3}u \,;\; V = \kappa^{-4}v ;\; P = \kappa^{-2}p$$

(12)

We assume that $\partial/\partial X, \partial/\partial Y, \partial/\partial \tau = 0(1)$ as $k \to 0$. Given that $U = 0(1)$, Equation (3) indicates that $V = 0(\kappa)$, We now let $p, \varphi_0 = 0\left(1/\kappa\right)$ as $k \to 0$.

We now assume the following expansion for the flow field:

$$\begin{aligned} U &= U_0 + \kappa^2 U_1 + \ldots \\ V &= V_0 + \kappa^2 V_1 + \ldots \\ P &= P_0 + \kappa^2 P_1 + \ldots \\ \varphi_0 &= \kappa^{-2}\varphi \end{aligned} \qquad (13)$$

The governing equation and the corresponding boundary conditions for the zero-order problem may be written as

$$\frac{\partial U_0}{\partial X} + \frac{\partial V_0}{\partial Y} = 0 \qquad (14)$$

$$n\left(\frac{\partial U_0}{\partial Y}\right)^{n-1} \frac{\partial^2 U_0}{\partial Y^2} = \frac{\partial P_0}{\partial X} + \frac{\partial \varphi_0}{\partial X} \qquad (15)$$

$$\frac{\partial P_0}{\partial Y} = 0 \qquad (16)$$

The boundary conditions are given by

$$Y = 0 : U_0 = V_0 = 0 \qquad (17)$$

$$Y = h ; \frac{\partial U_0}{2Y} = 0 ; P_0 = 3S\frac{\partial^2 h}{\partial x^2} - \frac{3S(a-h)}{a^2} ; \frac{\partial h}{\partial \tau} + U_0 \frac{\partial h}{\partial x} = V_0 \qquad (18)$$

The solutions for the velocity field are given by:

$$U_0 = \left[\frac{n}{n+1}\frac{\partial P_0'}{\partial X}^{1/n}\right]\left\{-(h-Y)^{(n+1)/n} + h^{(n+1)/n}\right\} \qquad (19)$$

$$\begin{aligned} V_o = &-\frac{1}{(n+1)}\frac{\partial P_0'}{\partial X}^{(1-n)/n}\frac{\partial^2 P_0'}{}\times \\ &\left[\frac{n}{2n+1}(h-Y)^{(2n+1)/n} + h^{(n+1)/n} Y - \frac{nh^{(2n+1)/n}}{(2n+1)}\right] \\ &+ \frac{n}{(n+1)}\frac{\partial P_0'}{\partial X}^{1/n}\frac{\partial h}{\partial X} \\ &\times\left\{h^{(n+1)/n} - \left((h-Y)^{(n+1)/n} + \frac{n+1}{n}h^{1/n} Y\right)\right\} \end{aligned} \qquad (20)$$

where,

$$P_0' = -(P_0 + \psi_0) \qquad (21)$$

$$P_0 = \left(-3S\frac{\partial^2 h}{\partial X^2} - \frac{3S(a-h)}{a^2}\right) \qquad (22)$$

Similarly, expressions u_1, v_1, and p_1 may be derived. These expressions are not used in the computations and they are very long. Therefore, they are not reproduced here. Using equations (14)-(22) and ignoring the curvature effect, we may show that the leading order evolution equation for the film rupture is given by:

$$\begin{aligned} \frac{\partial h}{\partial \tau} &+ \left\{3s\frac{\partial^3 h}{\partial X^3} + \frac{3A}{h^4}\frac{\partial h}{\partial X}\right\}^{1/n} h^{(n+1)/n}\frac{\partial h}{\partial X} = \\ &-\frac{1}{(2n+1)}\left(3S\frac{\partial^3 h}{\partial X^3} + \frac{3A}{h^4}\frac{\partial h}{\partial X}\right)^{(1-n)/n} \\ &\times\left(3S\frac{\partial^4 h}{\partial X^4} + 3A\frac{\partial}{\partial X}\left(\frac{1}{h^4}\frac{\partial h}{\partial X}\right)\right) h^{(2n+1)/n} \end{aligned} \qquad (23)$$

subject to initial conditions:

$$h(X,0) = f(x) \qquad (24)$$

Equation (23) governs long wave interfacial disturbances to the static film (having h=1) subject to van der Waals attractions.

3. Results and Discussion

The nonlinear partial differential equation (23) was solved numerically using an explicit marching numerical scheme. Central differences were used for space variable and the midpoint rule was used for time. The resulting system of difference equations was solved by the Lax-Wendroff technique. The Lax-Wendroff technique is an explicit, finite-difference method particularly suited to marching solutions. The problem was treated as an initial value problem with spatial periodic boundary conditions within the interval $0 < X < 2\pi/q$. In order to obtain a solution independent of the grid size, several computational runs were performed to seek the optimum step sizes for X and τ. The optimization procedure of the grid size includes computing the spatial film thickness distribution at an arbitrary time, employing a given number of grid points in spatial direction. After that, the number of grid points was increased gradually, each time; a computer run was performed to compute the film thickness profile. The procedure was continued until the absolute value of the difference in film thickness between two successive computer runs approached a value less than or equal to 10^{-6}. At this point, the spatial grid size was fixed. A similar procedure was followed to choose the optimum value for the time step. As a result of these computations, we used spatial grid points N=50 and time step $\Delta\tau = 0.001$ in all the computations.

The initial condition was given by:

$$h(X,0) = 1 + B\,Sin(qX) \tag{25}$$

We treated B, n, A and S as independent parameters. Figure 2 shows the initial disturbance introduced and the film profile at the time of film rapture. The break up area is larger in the case of the thicker film (c=4) at rupture time. Figure 7 shows the timewise variation of the minimum film thickness. At a given time, the minimum film thickness increases as n decreases. For pseudoplastic fluids, the film thickness is higher than the Newtonian case. For dilatant fluids, the film thickness is less than the Newtonian case. Figure 4 shows the rupture time versus the wave number of disturbance q. As the power law exponent for viscosity, "n" decreases, the rupture time increases at a given wave number of disturbance. The wave numbers of these most unstable modes are close to $1/2^{0.5}$. Figure 3 shows the variation of rupture time decreases as the disturbance amplitude increases. The results of Williams and Davis [8] and Sharma and Ruckenstein [5] are also displayed in Figure3. The agreement between our results and the published results is satisfactory.

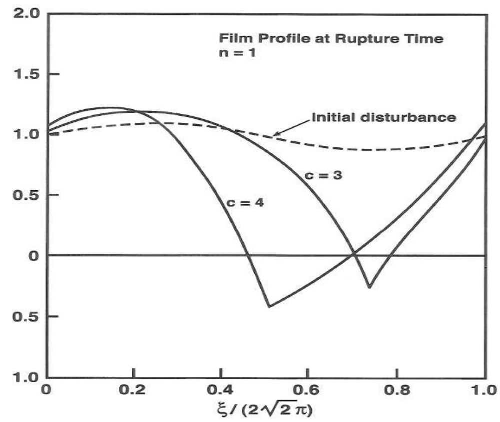

Figure 2: Film Thickness Distribution at the Rupture Time.

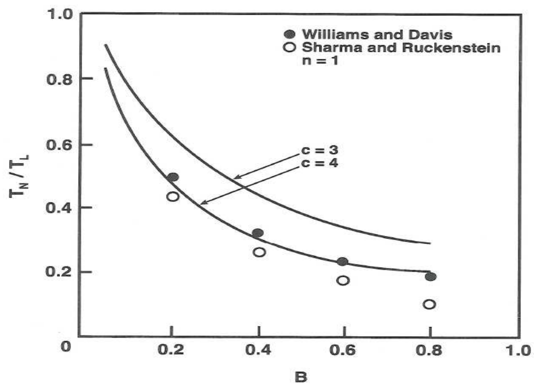

Figure 3: Minimum Film Thickness VS. Time.

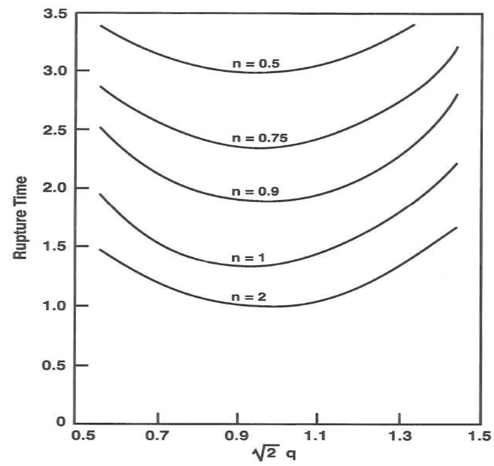

Figure 4: Rupture Time VS. q.

Figure 6 shows the results for rupture time in seconds as the initial amplitude of the disturbance B increases. We note that for pseudoplastic fluids (the power law index in less than 1); the rupture time is higher than the Newtonian fluid case at a given initial disturbance. Figure 5 shows the variation of the rupture time in seconds versus A. The rupture time decreases as A increases for a given type of viscosity power law index of the non-Newtonian fluid. As the value of “n’ decreases, the rupture time increases.

The model proposed in this paper does not take into account of the liquid film evaporation due to heat conduction from the corneal surface to the outer film interface or convective heat transfer from the ambient air above the saturation temperature at the interface. This will be undertaken in a future publication.

4. Conclusions

In this paper, we have investigated the rupture of a thin tear film. The Ostwald-de-Waele type power law model is employed for the mucous rheology. The van der Waals dispersion forces were included in the momentum equation. A nonlinear equation was derived for the tear film thickness based on lubrication approximation and long wave theory. Numerical solutions were obtained for the film thickness for a range of values of the Hamaker constant and power law exponent. The results indicate that the rheological properties, interfacial tension and the initial disturbance amplitude have significant effect on tear film rupture. Film rupture may be delayed by using anti-surfactant which increases the aqueous-mucus interfacial tension.

We have assumed that evaporation is minimal so that dry eye is caused by tear film volume deficiency. We plan to explore scenarios when evaporation is suspected of contributing to dry eye. This will be reported in a future publication.

Significant three dimensional flow effects occur in real eyes. The aqueous tear supply enters from the lacrimal glands at the top, outer part of the eye, and the tear film drains out at the bottom of the eye. The methodology presented in the paper could be used to examine tear film evolution in the presence of contact lens. Research into the effect slip on the tear film rupture time will be the subject of future work. Recent experimental evidence has suggested that the no slip condition may not be suitable for hydrophilic flows over hydrophobic boundaries at the micro and nano scales.

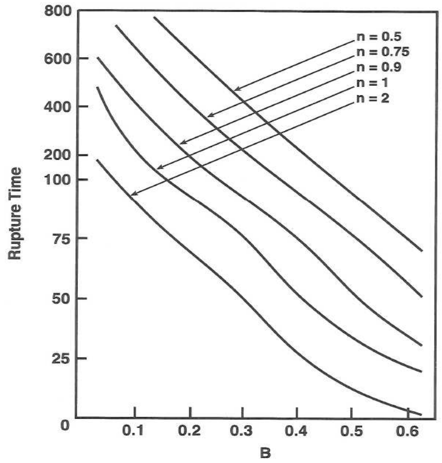

Figure 5: Ratio of Nonlinear to Linear Rupture Times VS. B

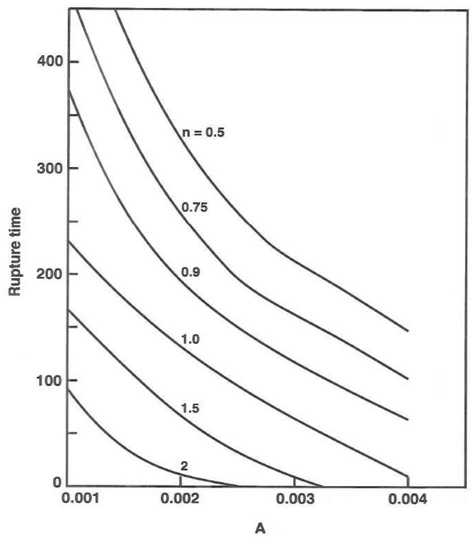

Figure 6: Rupture Time VS. B

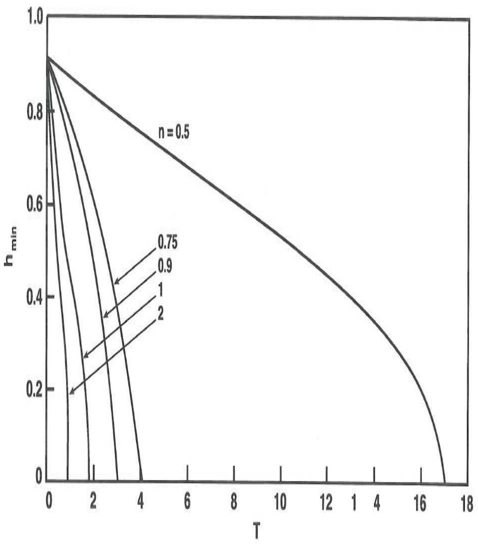

Figure 7: Rupture Time Versus A

References:

1. Holly, F.J., "Formation and Rupture of the Tear Film," Exp. Eye Research, Vol. 15, 1973, pp. 515-525.
2. Sharma, A., "Energetics of Corneal Epithelial Cell-ocular Mucus-tear Film Interactions: Some Surface Chemical Pathways of Corneal Defense," Biophysics. Chem., Vol. 47, 1993, pp. 87-99.
3. Lin, S.P., "Tear Film Rupture," Journal of Colloid Interface Science, Vol. 89, 1982, pp.226-231.
4. Sharma, A. and Ruckenstein, E., "Mechanism of Tear Film Rupture and Formation of Dry Spots on Cornea," Journal of Colloid Interface Science, Vol. 106, 1985, pp. 12-27.
5. Sharma, A. and Ruckenstein, E., "An Analytical Nonlinear Theory of Thin Film Rupture and its Application to Wetting Films," Journal of Colloid Interface Science, Vol. 113, 1986, pp. 456-479.
6. Sharma, A., Tiwari, S., Khanna, R. and Tiffany, J.M., "Hydrodynamics of Meniscus-induced Thinning of the Tear Film," Lacrimal Gland, Tear Film, and Dry Eye Syndromes 2, Plenum Press, New York, 1998.
7. Gorla, M.S.R. and Gorla, R.S.R., "Nonlinear Theory of Tear Film Rupture," Transactions of ASME, Journal of Biomechanical Engineering, Vol. 122, 2000, pp. 498-503.
8. Williams, M.B. and Davis, S.H., "Nonlinear Theory of Film Rupture," Journal of Colloid Interface Science, Vol. 90, 1982, pp. 220-228.
9. Lawrenson, J.G., Murphy, P.J. and Esmaeelpour, M., "The Neonatal Tear Film," Contact Les and Anterior Eye, Vol. 23, 2003, pp. 197-202.
10. Nichols, K.K., Nichols, J.J. and Mitchell, G.L., "The Relation Between Tear Film Tests in Patients with Dry Eye Disease," Opathalmology Physiology Opt., Vol. 23, 2003, pp. 553-560.